



Development of 3-substituted-1*H*-indole derivatives as NR2B/NMDA receptor antagonists

Rosaria Gitto^{a,*}, Laura De Luca^a, Stefania Ferro^a, Rita Citraro^b, Giovambattista De Sarro^b, Lara Costa^c, Lucia Ciranna^c, Alba Chimirri^a

^a Dipartimento Farmaco-Chimico, Università di Messina, Viale Annunziata, 98168 Messina, Italy

^b Dipartimento di Medicina Sperimentale e Clinica, Università Magna Graecia, Viale Europa Località Germaneto, 88100 Catanzaro, Italy

^c Dipartimento di Scienze Fisiologiche, Università di Catania, Viale Andrea Doria 6, 95125 Catania, Italy

ARTICLE INFO

Article history:

Received 8 September 2008

Revised 22 December 2008

Accepted 24 December 2008

Available online 31 December 2008

Keywords:

NR2B/NMDA antagonist

Molecular modeling

Anticonvulsant activity

Patch clamp

Binding affinity

ABSTRACT

A combined ligand-based and structure-based approach has previously allowed us to identify NR2B/NMDA receptor antagonists containing indole scaffold. In order to further explore the main structure activity relationships of this class of derivatives we herein report the design, synthesis and biological evaluation of new analogues. Some derivatives demonstrated to produce significant anticonvulsant properties and NMDA antagonism. The most active of them (**3d**) showed NR2B binding affinity equipotent to that of ifenprodil. These results were also corroborated by computational studies.

© 2008 Elsevier Ltd. All rights reserved.

1. Introduction

The evidence supporting a role of excessive glutamate release or receptor activation in pathological processes of Central Nervous System (CNS) led to the development of agents that modulate the glutamate transmission. NMDA receptors (NMDARs) belonging to the ionotropic glutamate receptor (iGluR) family are involved in many physiological processes, such as neuronal development, learning and memory but also play important roles in pathological states of CNS, including strokes, seizures, and pain.^{1–3} Functional NMDARs are heteromeric complexes containing NR1 and NR2 subunits (NR2A–D subtypes), and more rarely NR3 subunit. NR1 and NR2 subunits share a common membrane topology with other members of the iGluR family. Each subunit has a large extracellular amino-terminal domain (ATD), three transmembrane segments (M1, M3 and M4), a pore lining P-loop region (M2), an extracellular loop (L3) located between M3 and M4, and an intracellular carboxy terminal domain (CTD). It was demonstrated that the ATD is structurally similar to the bacterial periplasmic leucine, isoleucine, valine binding protein (LIVBP). Using molecular modelling and site-directed mutagenesis studies, it has been demonstrated that the LIVBP-like domain of the NR2B subunit contains the binding pocket for non-competitive NR2B-antagonists.^{4–6} The two proto-

typic NR2B subtype-selective antagonists, ifenprodil (**1**)^{7–16} and its more selective analogue Ro 25-6981 (**2**) (Chart 1), have good potential as neuroprotective agents and have been shown to bind at the so-called ifenprodil site.^{17,18}

Considering it has been established that NR2B/NMDA receptor may be playing a crucial role in epileptic disorders, in previous studies we reported a molecular modelling strategy that through a combined ligand-based and target-based approach led to the identification of new NR2B subtype-selective ligands containing an indole scaffold as anticonvulsant agents. In particular, compound **3a** (Chart 1), with the best binding data affinity, was able to prevent audiogenic seizures in DBA/2 mice and reduce NMDA receptor-mediated current in patch clamp experiments as well as exert a neuroprotective effect in HCN-1A.¹⁹

Starting from these promising results and considering the significant structural information obtained from our computational studies about NR2B subtype-selective ligands, we planned some modifications of compound **3a** as depicted in general formula **A** (Chart 1). Our investigations were generally aimed at clarifying the impact on the pharmacological effects of the following features: (i) benzene-fused ring substitution and modification (R and Y); (ii) the nature of the X spacer; (iii) the presence of another positive ionizable group (Z) on the benzylpiperidine moiety. All the synthesized compounds were tested in order to evaluate their anticonvulsant properties in DBA/2 mice and the binding and functional activity of the most active derivatives were also studied.

* Corresponding author. Tel.: +39 0906766413; fax: +39 0906766402.

E-mail address: rgitto@pharma.unime.it (R. Gitto).

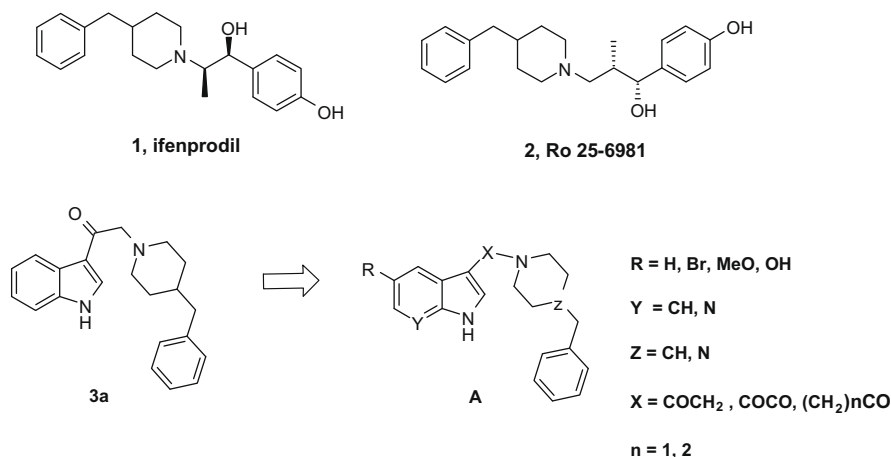


Chart 1. NR2B/NMDA antagonists and planned modifications.

Moreover, docking simulations were carried out to rationalize the biological results.

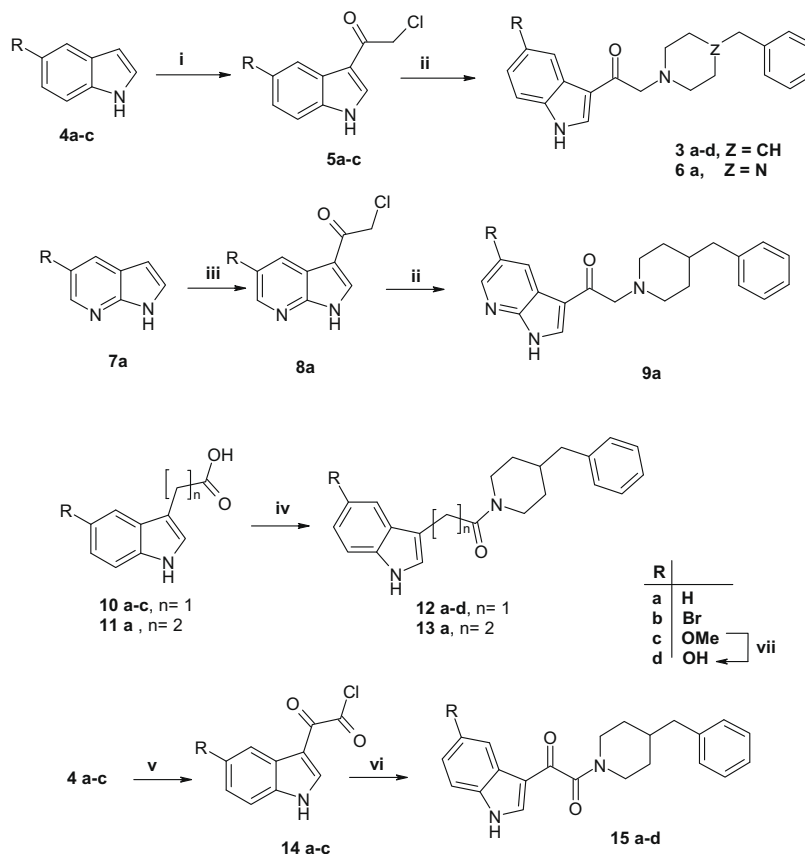
2. Results and discussion

2.1. Synthesis

The synthetic pathways employed to obtain the designed indole derivatives are depicted in Scheme 1. Following a previously reported method¹⁹ starting from compounds **4a–c**, we prepared 2-chloro-1-(1*H*-indol-3-yl)ethanones **5a–c**, which were converted

into the corresponding derivatives **3a–c** and **6a** by reaction with 4-benzylpiperidine and benzylpiperazine; similarly, the 2-(4-benzylpiperidin-1-yl)-1-(1*H*-pyrrolo[2,3-*b*]pyridin-3-yl)ethanone **9a** was prepared from chloroacetyl intermediate **8a** in turn obtained from 7-azaindole **7a** by treatment with chloroacetyl chloride in the presence of AlCl₃ as catalyst. By using a standard amide coupling reaction with 4-benzylpiperidine the 2-(1*H*-indol-3-yl)-2-acetic acids **10a–c** and 3-(1*H*-indol-3-yl)propanoic acid **11a** gave compounds **12a–c** and **13a**, respectively.

Due to the high nucleophilic character at the 3-position of indole, the treatment with oxalyl chloride of appropriate substituted



Scheme 1. Reagents and conditions: (i) ClCH₂COCl, pyridine, dioxane, Δ, 2 h; (ii) 4-benzylpiperidine or benzylpiperazine, K₂CO₃, toluene, Δ, 3 h; (iii) ClCH₂COCl, AlCl₃, DCM, rt, 3 h; (iv) 4-benzylpiperidine, HBTU, TEA, DMF, rt 2 h; (v) ClCOCOCl, diethyl ether, rt, 2 h; (vi) 4-benzylpiperidine, THF, TEA, rt, 2 h; (vii) BBr₃ (1.0 M DCM), rt, 10 h.

indoles **4a–c** produced the corresponding 2-(1*H*-indol-3-yl)-2-oxoacetyl chloride intermediates **14a–c** which were then coupled with 4-benzylpiperidine in alkaline medium in a one-pot procedure to give the desired 1-(4-benzylpiperidin-1-yl)-2-(1*H*-indol-3-yl)ethane-1,2-diones (**15a–c**). Finally, by treatment with boron tribromide solution (1.0 M in methylene chloride) compounds **3c**, **12c**, and **15c** were demethylated into the corresponding hydroxyl-derivatives **3d**, **12d**, and **15d**. The structures of all compounds obtained were supported by elemental analyses and spectroscopic measurements.

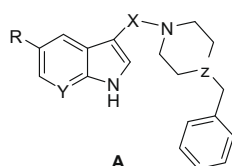
2.2. Anticonvulsant properties

Initially, we examined the impact on anticonvulsant properties of the planned structural modifications by introducing new substituents and moieties on the 'hit compound' **3a**, which had shown good *in vivo* activity. The anticonvulsant effects of indole derivatives **3a–d**, **9a**, **12a–d**, **13a**, and **15a–d** were evaluated against audiogenic seizures in DBA/2 mice, which has been considered an excellent animal model for generalized epilepsy and for screening new anticonvulsant drugs.²⁰ The results were compared with those of the NMDA/NR2B receptor antagonist Ro 25-6981 (**2**), and the ED₅₀ values after intraperitoneal (ip) administration are presented in Table 1. The pharmacological results obtained highlighted some structure–activity relationship considerations for this class of compounds. The presence of bromine (**3b**) or methoxy group (**3c**) in position 5 of the benzene-fused ring of 'hit compound' **3a** negatively influences anticonvulsant efficacy. On the contrary, the introduction of a hydroxyl-substituent in the same position led to an improvement of anticonvulsant properties so that compound **3d** was two-fold more active than the corresponding unsubstituted derivative **3a** and ~4-fold that of Ro 25-6981 (**2**).

The 4-benzylpiperidine moiety of the reference compound **3a** was replaced with the benzylpiperazine group, but this modification produced the inactive derivative **6a**, probably indicating that the presence of a supplementary positive charge is not conducive to pharmacological activity. We also substituted the benzene-fused ring of compound **3a** with a pyridine nucleus and the obtained analogue **9a** showed a significant decrease in the anticonvulsant properties. As regards the effect of linker modifications, in terms of both the inversion of the position of carbonyl group and the length of the spacer, we obtained the following results. Compounds **12a–d**, in which the carbonyl function was directly linked to the nitrogen atom of the 4-benzylpiperidine moiety, generally proved to be less active than the corresponding compounds **3a–d**, with exception of derivative **12b** that protected against seizures showing ED₅₀ values of the same order of magnitude as the 'hit compound' **3a**. Finally, to confirm the crucial role of the distance between the positive ionizable nitrogen atom and indole fragment, the alkyl chain of hit compound **3a** was lengthened; this modification did not appear to promote activity as it produced the inactive compound **13a**. Moreover, we introduced a further carbonyl group in the spacer via the replacement of acetyl linker with an oxalyl fragment for compounds **15a–d**; although compound **15a** showed similar activity against audiogenic seizures when compared with parent compound **3a**, surprisingly the **15a** analogues, bearing other substituents such as bromine, methoxy, and also a hydroxyl group (**15b–d**) did not display *in vivo* efficacy.

In attempt to find a correlation between the physico-chemical properties of the tested compounds and the rank order of anticonvulsant efficacy, we estimated their relative lipophilicity (log*D*_{7.4}).²¹ However, the different degree of the potency generally did not seem to be directly related to the log*D*_{7.4} values (see Table 1), thus suggesting the influence of other parameters.

Table 1
Anticonvulsant activity of indole derivatives against audiogenic seizures in DBA/2 mice and prediction of their log*D*_{7.4} values



	R	Y	X	Z	ED ₅₀ μmol/kg ^a		Log <i>D</i> _{7.4} ^b
					Clonus	Tonus	
3a^c	H	CH	COCH ₂	CH	22.4 (13.9–36.2)	8.71 (5.71–13.3)	4.73
3b^c	Br	CH	COCH ₂	CH	84.9 (64.7–111)	49.7 (34.8–71.0)	5.86
3c^c	OMe	CH	COCH ₂	CH	59.9 (38.7–92.7)	36.5 (26.1–51.0)	4.90
3d	OH	CH	COCH ₂	CH	11.5 (7.96–16.5)	6.48 (4.56–9.21)	3.81
6a	H	CH	COCH ₂	N	>100	>100	3.08
9a	H	N	COCH ₂	CH	88.5 (52.5–149)	32.5 (22.8–46.4)	4.85
12a	H	CH	CH ₂ CO	CH	70.3 (53.3–92.9)	39.2 (20.5–77.8)	4.36
12b	Br	CH	CH ₂ CO	CH	27.3 (15.4–48.2)	5.42 (2.08–14.1)	5.21
12c	OMe	CH	CH ₂ CO	CH	89.0 (59.9–132)	34.4 (21.3–69.1)	4.27
12d	OH	CH	CH ₂ CO	CH	45.6 (23.4–89.2)	13.9 (11.2–17.1)	3.18
13a	H	CH	(CH ₂) ₂ CO	CH	>100	57.6 (38.4–86.4)	4.87
15a	H	CH	COCO	CH	22.4 (10.9–45.9)	0.95 (0.26–3.52)	3.28
15b	Br	CH	COCO	CH	>100	47.9 (28.1–81.7)	4.14
15c	OMe	CH	COCO	CH	>100	78.8 (53.7–116)	3.20
15d	OH	CH	COCO	CH	>100	>100	2.11
2	—	—	—	—	40.0 (21.1–54.7)	10.6 (5.16–21.8)	—

^a All data were calculated following the Litchfield and Wilcoxon method. At least 32 animals were used to calculate each ED₅₀ 95% confidence limits are given in parentheses.

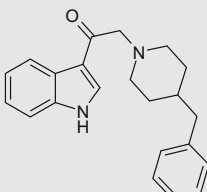
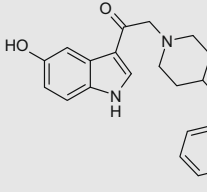
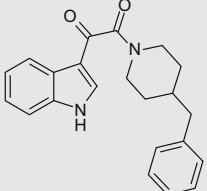
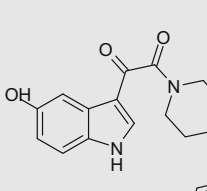
^b Log*D* data at pH 7.4 are predicted from a commercially available programme (ACD/Lab).²¹

^c Ref. 19.

2.3. Binding affinity

On the basis of the anticonvulsant efficacy and in order to investigate the mechanism of action we evaluated the ability of some selected compounds to interact with the NMDA/NR2B receptor by testing [^3H]ifenprodil binding inhibition (Table 2) in Wistar rat cerebral cortex following a reported procedure (see Section 4). Compound **3d**, for which the highest binding affinity was found with an IC_{50} of 0.025 μM (see Table 2), showed a 30-fold improvement over the parent compound **3a** and a potency comparable to that of ifenprodil (**1**). Figure 1 displays the inhibition of [^3H]ifenprodil in the binding assay; the response curve for the most potent ligand **3d** ($\text{IC}_{50} = 0.025 \mu\text{M}$, $K_i = 0.023 \mu\text{M}$) is very similar to that for the reference compound ifenprodil (**1**) ($\text{IC}_{50} = 0.0205 \mu\text{M}$, $K_i = 0.019 \mu\text{M}$) at different doses. This result suggests that the introduction of the 5-hydroxyl group onto the benzene-fused ring positively influences the binding affinity. When testing the binding affinity of the oxalyl-analogues **15a** and **15d**, we observed a significant decrease in NR2B binding affinity when compared with that of **3a** and **3d**; as expected, a moderate affinity re-emerged in the 5-hydroxyl substituted derivative **15d**, although it was inactive in the in vivo pharmacological evaluation (see Table 1). From these results we speculated that the presence of a 5-hydroxyl group coupled with a basic amine centre might optimize the NR2B binding affinity for this class of compounds.

Table 2
Structure and binding affinity^a of ifenprodil and selected indoles

		$\text{IC}_{50}\%$ at 10 μM	IC_{50} (μM)
3a		89	0.769
3d		92	0.0250
15a		36	N.D.
15d		77	2.66
1	Ifenprodil	—	0.0205

^a Displacement of [^3H]ifenprodil.²⁵ N.D. = not detectable.

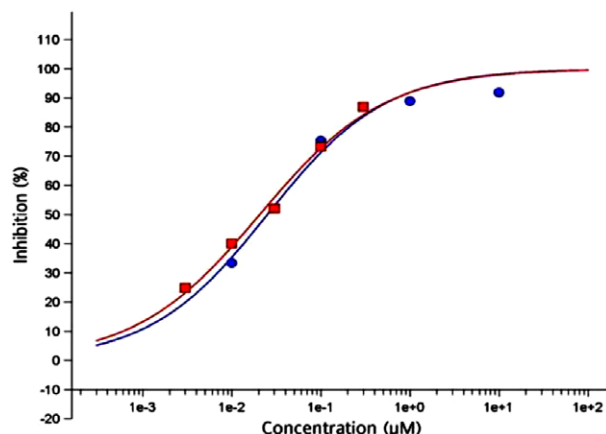


Figure 1. Inhibition of [^3H]ifenprodil binding to Wistar rat cerebral cortex²² by **3d** (blue circles) and ifenprodil (**1**) (red squares).

2.4. Electrophysiological studies

Subsequently, we focused our attention on the 2-(4-benzylpiperidin-1-yl)-1-(5-hydroxy-1*H*-indol-3-yl)ethanone (**3d**), which demonstrated the highest anticonvulsant activity and NR2B ifenprodil-site receptor binding affinity. With the aim of studying its mechanism of action, a patch clamp study was also performed on brain slices from rat hippocampus, prepared as described previously.²² Membrane currents were recorded from single CA1 pyramidal neurons at a holding potential of -60 mV ; application of NMDA (50 μM , 5 s) together with glycine (0.5 μM) evoked an inward current, the amplitude of which ranged between 110 and 998 pA in different neurons (Fig. 2A and B). Following continuous application of compound **3d** (10 μM , 5 min) through the perfusion system, the amplitude of NMDA-mediated current was reduced (Fig. 2A and B). The effect of **3d** was dose dependent: at 1 μM concentration the amount of inhibition was statistically significant in 1 out of 4 cases whereas higher concentrations (10 and 100 μM) induced a significant inhibition in the majority of neurons tested (5 out of 7, Fig. 2B). Percent reduction values of NMDA-mediated current by compound **3d** at 1, 10 and 100 μM concentrations were, respectively, 23 ± 9 , 52 ± 10 and 75 (mean \pm SEM, $n = 4, 5$ and 1; Fig. 2C). The effect of **3d** was reversible; the amplitude of NMDA-mediated current returned to control values within 10 min after the end of **3d** application (Fig. 2D).

These results indicate that compound **3d** behaved as an antagonist of NMDA receptors, exerting a dose-dependent and reversible inhibition of NMDA-mediated current.

2.5. Docking studies

Docking simulations were carried out in order to rationalize the obtained findings for this class of compounds. In our previous studies¹⁹ we modelled the structure of NR2B/ifenprodil-like binding domain and highlighted the binding mode of 'hit compound' **3a** in the binding pocket (Fig. 3). The main contact observed was the electrostatic interaction between the protonated nitrogen atom of the ligand and the carboxyl group of aspartate D101, which previous site-directed mutagenesis studies⁵ had highlighted as being crucial for NR2B interaction. Moreover, compound **3a** was involved not only in an H bonding interaction between the indole ring NH and residue E235, but also in hydrophobic interactions with some specific residues (T233, V42, L261, A263, H127, A298, I297 and F176). Notably, the binding pose of the new identified 'hit compound' **3d** was very similar to the one previously reported for reference compound **3a** but, as shown

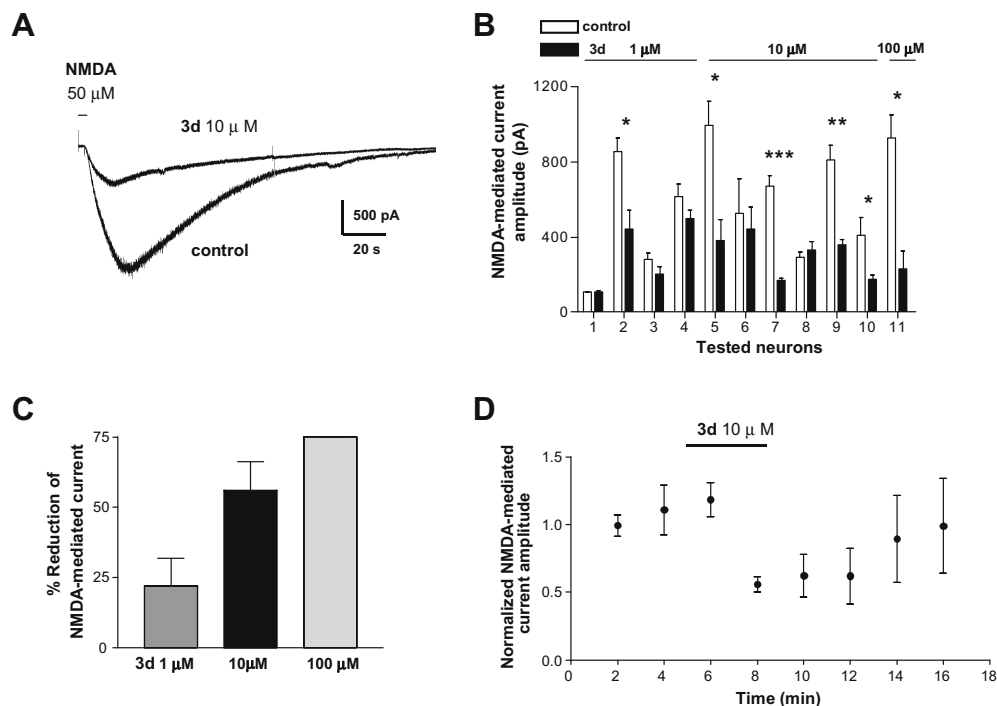


Figure 2. Inhibition of NMDA-mediated current by compound **3d**. (A) Patch clamp recording of membrane ion currents from a single CA1 pyramidal neuron (HP -60 mV) of rat hippocampus: application of NMDA ($50 \mu\text{M}$, 5 s) induced an inward current, the amplitude of which was strongly reduced during bath perfusion of compound **3d** ($10 \mu\text{M}$, 5 min). (B) The amplitude of NMDA-mediated current (mean \pm SEM of at least three consecutive responses) in the presence of **3d** (filled columns) was significantly decreased with respect to control conditions (empty columns) in most of the neurons examined ($^{***}P < 0.0001$; $^{**}P < 0.001$; $^{*}P < 0.01$; student's unpaired t -test, two-tailed). (C) The amount of inhibition of NMDA-mediated current increased with concentration of compound **3d** (1 , 10 and $100 \mu\text{M}$). (D) Normalized amplitude values of NMDA-mediated currents in different neurons were averaged (mean \pm SEM, $n = 6$) and represented as a function of time. Inhibition of NMDA-mediated current by **3d** ($10 \mu\text{M}$, 5 min) was reversible: recovery was observed within 10 min after washout.

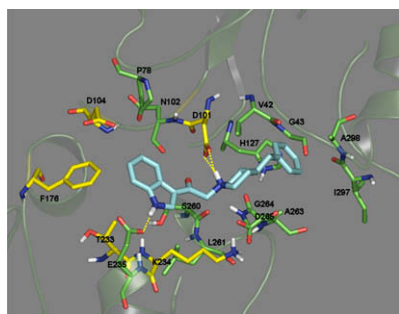


Figure 3. Docking model of compound **3a** (cyan) at the modelled binding pocket. The most important residues identified by mutagenesis-site directed studies⁵ are depicted in yellow.

in Figure 4A, the presence of a 5-hydroxyl group on the indole scaffold of **3d** generates the possibility of a new contact as hydrogen bonding with the important residue D104. Considering the reported mutations results⁵ this new contact could lead to more favourable interactions within the binding pocket and provide a possible explanation for the improvement of the binding affinity observed for compound **3d**, which resulted 30-fold more potent with respect to parent compound **3a** (see Table 2). In an attempt to explain the poor in vitro efficacy of compound **15d** we studied its binding pose (Fig. 4B) in comparison with that shown by analogue **3d**. We mainly observed that the less active compound **15d**, lacking positive ionizable nitrogen atom, did not show any electrostatic interaction with the carboxyl group of residue D101. However, it did maintain the hydrophobic contacts and the favourable H-bonding interaction with residue E235 observed also for derivative **3d**. The GOLD fitness score of the best docking solu-

tions for **3d** and **15d** (65.77 and 60.86, respectively) also correlated with their IC_{50} binding affinity. These findings could justify the data binding affinity of compound **15d** and simultaneously confirmed that our modelled binding pocket would be able to predict the ranking order of ligand potency of to binding recognition sites for this class of compounds.

3. Conclusions

In an attempt to carefully investigate the structure–activity relationships of new NR2B/antagonists containing indole nucleus, a set of 3-substituted derivatives were synthesized and tested. Some of them demonstrated anticonvulsant properties against audiogenic seizures in DBA2/mice. In particular, the compound **3d** with the best in vivo pharmacological profile also showed the highest binding affinity to NR2B ifenprodil-like receptor subunits. Notably, we found that the activity of compound **3d** was better than **3a** and that it was equipotent to ifenprodil (**1**) in 'in vitro' test. These results were supported by our docking studies, which clarified its good interaction into the binding pocket.

Moreover, by electrophysiology studies we found that compound **3d** was able to reduce NMDA receptor-mediated current in CA1 pyramidal neurons from rat hippocampus, suggesting that it could be considered a new potent antagonist of NR2B/NMDA receptors and might be useful as a neuroprotective agent.

4. Experimental

4.1. Chemical experiments

Melting points were determined on a Stuart SMP10 apparatus and are uncorrected. Elemental analyses (C, H, N) were carried

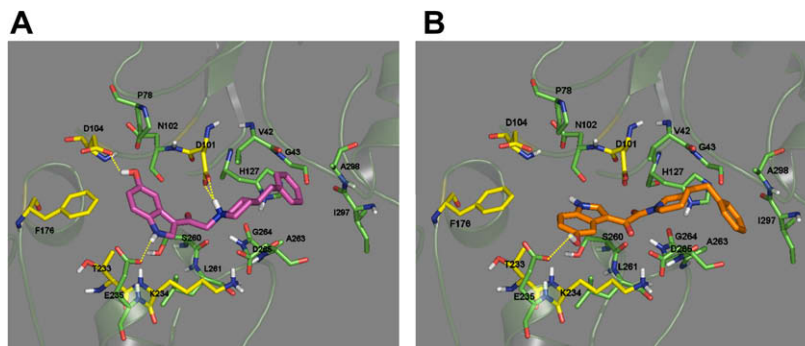


Figure 4. The best docked conformations of compounds **3d** (4A) and **15d** (4B) at the modelled binding pocket. The most important residues identified by mutagenesis-site directed studies⁵ are depicted in yellow.

out on a Carlo Erba Model 1106 Elemental Analyzer and the results are within $\pm 0.4\%$ of the theoretical values. Merck silica gel 60 F₂₅₄ plates were used for analytical TLC; column chromatography was performed on Merck silica gel 60 (70–230 mesh). Flash chromatography (FC) was carried out on a Biotage SP4 EXP. ¹H NMR spectra were measured in CDCl₃ or dimethylsulphoxide-*d*₆ (DMSO-*d*₆) with a Varian Gemini 300 spectrometer; chemical shifts are expressed in δ (ppm) and coupling constants (*J*) in Hz. All exchangeable protons were confirmed by addition of D₂O. GC–MS spectra for selected compounds were recorded on a Shimadzu QP500 EI 151 mass spectrometer.

4.1.1. Synthesis of 2-(4-benzylpiperidin-1-yl)-1-(5-hydroxy-1*H*-indol-3-yl)ethanone (**3d**)

Derivative **3c** (0.001 mol), which was synthesized from compound **5c** as previously reported,¹⁹ was dissolved in methylene chloride (DCM) (5 mL), treated with BBr₃ (1 M in DCM) (6 mL, 0.006 mol) and stirred overnight. Successively, methanol (7 mL) was carefully added at 0 °C and the solvents removed under reduced pressure. The residue was dissolved in ethyl acetate (10 mL) and washed with water (10 mL \times 3). The organic layer was dried (Na₂SO₄), combined and concentrated in vacuo. The crude product was crystallized from ethanol to give the desired compound **3d**. Yield 68%. Mp 214 °C dec. ¹H NMR (DMSO-*d*₆) 1.14–3.24 (m, 11H), 3.33 (s, 2H, CH₂N), 6.68–7.56 (m, 8H, ArH), 8.33 (s, 1H, H-2), 9.00 (s, 1H, OH), 11.66 (br s, 1H, NH). Anal. Calcd for C₂₂H₂₄N₂O₂: C, 75.83; H, 6.94; N, 8.04. Found: C, 75.89; H, 6.85; N, 8.15.

4.1.2. Synthesis of 2-(4-benzylpiperazin-1-yl)-1-(1*H*-indol-3-yl)ethanone (**6a**)

A solution of 3-chloroacetylindole derivative (**5a**, 0.001 mol), previously reported by us,¹⁹ benzylpiperazine (0.001 mol) and K₂CO₃ (0.0005 mol) was refluxed in toluene (5 mL) for 3 h. The organic phase was filtered and, after removal of the solvent under reduced pressure, the residue was powdered by treatment with diethyl ether and recrystallized from EtOH to give the desired compound (**6a**). Yield 49%. Mp 192 °C dec. ¹H NMR (CDCl₃) 2.55–2.65 (m, 8H), 3.53 and 3.64 (2s, 4H, CH₂), 7.25–7.43 (m, 8H, ArH), 8.31 (s, 1H, H-2), 8.40 (br s, 1H, H-4), 8.66 (br s, 1H, NH). GC–MS (EI) *m/z* (%): 333 (M⁺, 12), 190 (14), 189 (100), 175 (13), 146 (9), 91 (34). Anal. Calcd for C₂₁H₂₃N₃O: C, 75.65; H, 6.95; N, 12.60. Found: C, 75.72; H, 6.68; N, 12.40.

4.1.3. Synthesis of 2-(4-benzylpiperidin-1-yl)-1-(1*H*-pyrrolo[2,3-*b*]pyridin-3-yl)ethanone (**9a**)

A suspension of 7-azaindole (**7a**) (0.001 mol) and AlCl₃ (0.005 mol) in methylene chloride (5 mL) was stirred at room temperature for 1 h, then a solution of chloroacetyl chloride

(0.005 mol) in the same solvent (2 mL) was added dropwise.²³ The reaction mixture was stirred for 2 h, then methanol (5 mL) was carefully added at 0 °C and the solvent removed under reduced pressure. A saturated aqueous NaHCO₃ solution (5 mL) was added and the reaction mixture was extracted with ethyl acetate. The organic phase was dried over Na₂SO₄ and the solvent removed under reduced pressure to give a crude residue; by treatment of residue with diethyl ether the intermediate 2-chloro-1-(1*H*-pyrrolo[2,3-*b*]pyridin-3-yl)ethanone (**8a**) was obtained. Subsequently derivative **8a** (0.001 mol), benzylpiperidine (175 mg, 0.001 mol) and K₂CO₃ (0.0005 mol) were refluxed in toluene (5 mL) for 3 h. The organic phase was filtered and, after removal of the solvent under reduced pressure, the residue was powdered by treatment with diethyl ether and recrystallized from ethanol to give the desired compound **9a**. ¹H NMR spectral data confirmed the structure of intermediate **8a** and were in accordance with the literature.²³ Yield 42%. Mp 151 °C dec. ¹H NMR (DMSO-*d*₆) 1.37–3.00 (m, 9H), 2.52 (d, 2H, *J* = 6.84, CH₂Ph), 3.59 (s, 2H, CH₂N), 7.13–8.72 (m, 9H, ArH), 10.95 (br s, 1H, NH). GC–MS (EI) *m/z* (%): 333 (M⁺, 0.5), 189 (17), 188 (100), 174 (17), 145 (18), 91 (22). Anal. Calcd for C₂₁H₂₃N₃O: C, 75.65; H, 6.95; N, 12.60. Found: C, 75.44; H, 6.70; N, 12.88.

4.1.4. General procedure for the synthesis of 1-(4-benzylpiperidin-1-yl)-2-(1*H*-indol-3-yl)ethanones (**12a–c**) and 1-(4-benzylpiperidin-1-yl)-3-(1*H*-indol-3-yl)propan-1-one (**13a**)

A mixture of 2-(1*H*-indol-3-yl)acetic acid (**10a–c**) or 3-(1*H*-indol-3-yl)propanoic acid (**11a**) (0.001 mol) with *N,N,N,N*-tetramethyl-*O*-(1*H*-benzotriazol-1-yl)uronium hexafluorophosphate (HBTU) in dimethylformamide (2 mL) was stirred for 30 min at room temperature. Successively, 4-benzylpiperidine (0.001 mol) and catalytic amount of triethylamine were added, the mixture was stirred for 2 h at room temperature. The reaction mixture was then quenched with water (10 mL) and extracted with ethyl acetate. The combined extracts were dried with dry Na₂SO₄ and concentrated in vacuo. The crude compound was crystallized by treatment with ethanol to give the desired final products (**12a–c** and **13a**).

4.1.4.1. 1-(4-Benzylpiperidin-1-yl)-2-(1*H*-indol-3-yl)ethanone (**12a**)

Yield 82%. Mp 54–55 °C ¹H NMR (CDCl₃) 0.94–4.66 (m, 9H), 2.49 (mc, 2H, CH₂Ph), 3.83 (s, 2H, CH₂), 7.07–7.64 (m, 10H, ArH), 8.07 (br s, 1H, NH). GC–MS (EI) *m/z* (%): 332 (M⁺, 53), 215 (8), 202 (13), 187 (6), 174 (3), 130 (100), 91 (20). Anal. Calcd for C₂₂H₂₄N₂O: C, 79.48; H, 7.28; N, 8.43. Found: C, 79.55; H, 7.40; N, 8.21.

4.1.4.2. 1-(4-Benzylpiperidin-1-yl)-2-(5-bromo-1*H*-indol-3-yl)ethanone (**12b**)

Yield 75%. Mp 72–74 °C ¹H NMR (DMSO-*d*₆) 0.90–4.34 (m, 9H), 2.42 (d, 2H, *J* = 7.26, CH₂Ph), 3.71 (s, 2H, CH₂), 7.10–

7.72 (m, 9H, ArH), 11.09 (br s, 1H, NH). Anal. Calcd for $C_{22}H_{23}BrN_2O$: C, 64.24; H, 5.64; N, 6.81. Found: C, 64.20; H, 5.66; N, 6.83.

4.1.4.3. 1-(4-Benzylpiperidin-1-yl)-2-(5-methoxy-1H-indol-3-yl)ethanone (12c). Yield 96%. Mp 60–62 °C. 1H NMR ($CDCl_3$) 0.96–4.70 (m, 9H), 2.55 (mc, 2H, CH_2Ph), 3.91 (s, 3H, MeO), 3.84 (s, 2H, CH_2), 6.89–7.38 (m, 9H, ArH), 8.02 (br s, 1H, NH). Anal. Calcd for $C_{23}H_{26}N_2O_2$: C, 76.21; H, 7.23; N, 7.73. Found: C, 76.44; H, 7.00; N, 7.55.

4.1.4.4. 1-(4-Benzylpiperidin-1-yl)-3-(1H-indol-3-yl)propan-1-one (13a). Yield 35%. Mp 40–42 °C. 1H NMR ($DMSO-d_6$) 0.89–4.70 (m, 15H), 7.02–7.62 (m, 10H, ArH), 8.00 (br s, 1H, NH). GC–MS (EI) m/z (%): 346 (M^+ , 100), 216 (27), 174 (42), 143 (64), 13 (79), 117 (19), 91 (17). Anal. Calcd for $C_{23}H_{26}N_2O$: C, 79.73; H, 7.56; N, 8.09. Found: C, 79.80; H, 7.66; N, 8.20.

4.1.5. Synthesis of 1-(4-benzylpiperidin-1-yl)-2-(5-hydroxy-1H-indol-3-yl)ethanone (12d)

Compound **12d** was synthesized starting from derivative **12c** using the same procedure employed to prepare derivative **3d**. Yield 36%. Mp 187–88 °C. 1H NMR ($DMSO-d_6$) 0.89–4.35 (m, 9H), 2.42 (d, 2H, $J = 7.26$, CH_2Ph), 3.61 (s, 2H, CH_2CO), 6.55–7.27 (m, 9H, ArH), 8.57 (s, 1H, OH), 10.54 (br s, 1H, NH). Anal. Calcd for $C_{22}H_{24}N_2O_2$: C, 75.83; H, 6.94; N, 8.04. Found: C, 75.85; H, 6.99; N, 8.11.

4.1.6. General procedure for the synthesis of 1-(4-benzylpiperidin-1-yl)-2-(1H-indol-3-yl)ethane-1,2-diones (15a–c)

Oxalyl chloride (0.175 mL, 0.002 mol) was added dropwise at 0 °C to a solution of appropriate indole (0.001 mol) in diethyl ether (5 mL), under N_2 atmosphere. The reaction mixture was stirred at the same temperature for 2 h; this was followed by concentration in vacuo to remove the diethyl ether. To a solution in tetrahydrofuran (5 mL) of the crude material obtained in previous 4-benzylpiperidine (175 mg, 0.001 mol) and catalytic amount of triethylamine were added, the mixture was stirred for 2 h at room temperature. A saturated aqueous $NaHCO_3$ solution (5 mL) was added to quench the reaction and the mixture was extracted with ethyl acetate. The combined extracts were dried with dry Na_2SO_4 and concentrated in vacuo. The crude compound was purified by flash chromatography (FC) (cyclohexane/ethyl acetate, 1:1).

4.1.6.1. 1-(4-Benzylpiperidin-1-yl)-2-(1H-indol-3-yl)ethane-1,2-dione (15a). Yield 45%. Mp 187–188 °C. 1H NMR ($CDCl_3$) 1.25–4.63 (m, 9H), 2.55 (d, 2H, $J = 6.87$), 7.11–7.40 (m, 8H, ArH), 7.78 (s, 1H, H-2), 8.31 (br s, 1H, H-4), 9.50 (br s, 1H, NH). GC–MS (EI) m/z (%): 346 (M^+ , 10), 174 (16), 144 (100), 91 (10). Anal. Calcd for $C_{22}H_{22}N_2O_2$: C, 76.28; H, 6.40; N, 8.09. Found: C, 76.30; H, 6.41; N, 8.19.

4.1.6.2. 1-(4-Benzylpiperidin-1-yl)-2-(5-bromo-1H-indol-3-yl)ethane-1,2-dione (15b). Yield 48%. Mp 73–75 °C. 1H NMR ($CDCl_3$) 1.25–4.60 (m, 9H), 2.56 (d, 2H, $J = 6.87$), 7.11–7.35 (m, 7H, ArH), 7.66 (s, 1H, H-2), 8.44 (br s, 1H, H-4), 10.05 (br s, 1H, NH). Anal. Calcd for $C_{22}H_{21}BrN_2O_2$: C, 62.13; H, 4.98; N, 6.59. Found: C, 62.15; H, 4.77; N, 6.66.

4.1.6.3. 1-(4-Benzylpiperidin-1-yl)-2-(5-methoxy-1H-indol-3-yl)ethane-1,2-dione (15c). Yield 58%. Mp 92–94 °C. 1H NMR ($CDCl_3$) 1.25–4.63 (m, 9H), 2.56 (d, 2H, $J = 6.87$), 3.89 (s, 3H, MeO), 6.90–7.30 (m, 7H, ArH), 7.76 (s, 1H, H-2), 7.81 (br s, 1H, H-4), 9.20 (br s, 1H, NH). Anal. Calcd for $C_{23}H_{24}N_2O_3$: C, 73.38; H, 6.43; N, 7.44. Found: C, 73.43; H, 6.58; N, 7.60.

4.1.7. Synthesis of 1-(4-benzylpiperidin-1-yl)-2-(5-hydroxy-1H-indol-3-yl)ethane-1,2-dione (15d)

Compound **15d** was prepared following the same procedure employed for compound **3d** using 1-(4-benzylpiperidin-1-yl)-2-(5-methoxy-1H-indol-3-yl)ethane-1,2-dione **15c** as starting material. Yield 59%. Mp 140–142 °C. 1H NMR ($DMSO-d_6$) 1.02–4.39 (m, 9H), 2.52 (s, 2H, CH_2Ph), 6.71–7.47 (m, 8H, ArH), 7.94 (s, 1H, H-2), 9.13 (s, 1H, OH), 12.01 (br s, 1H, NH). Anal. Calcd for $C_{22}H_{22}N_2O_3$: C, 72.91; H, 6.12; N, 7.73. Found: C, 72.88; H, 6.21; N, 7.50.

4.2. Pharmacology testing of anticonvulsant activity

All experiments were performed with DBA/2 mice which are genetically susceptible to sound-induced seizures. DBA/2 mice (8–12 g; 22–25-day-old) were purchased from Harlan Italy (Corezzano, Italy). Groups of 10 mice of either sex were exposed to auditory stimulation 30 min following administration of either the vehicle or each dose of the drugs studied.²⁰ The compounds were administered intraperitoneally (ip) (0.1 mL/10 g of mouse body weight) as a freshly-prepared solution in 50% dimethylsulphoxide (DMSO) and 50% sterile saline (0.9% NaCl). Individual mice were placed under a hemispheric perspex dome (diameter 58 cm), and 60 s were allowed for habituation and assessment of locomotor activity. Auditory stimulation (12–16 kHz, 109 dB) was applied for 60 s or until tonic extension occurred, and induced a sequential seizure response in control DBA/2 mice, consisting of an early wild running phase, followed by generalized myoclonus and tonic flexion and extension sometimes followed by respiratory arrest. The control and drug-treated mice were scored for latency to and incidence of the different phases of the seizures. The experimental protocol and all the procedures involving animals and their care were conducted in conformity with the institutional guidelines and the European Council Directive of laws and policies.

4.3. Statistical analysis

Statistical comparisons between groups of control and drug-treated animals were made using Fisher's exact probability test (incidence of the seizure phases). The ED_{50} values of each phase of audiogenic seizures were determined for each dose of the compound administered, and dose–response curves were fitted using a computer programme by Litchfield and Wilcoxon's method.²⁴

4.4. Receptor binding studies

The radioligand binding assays were carried out using [3H]ifenprodil (Custom Screen by MDS pharma services, Taiwan).²⁵

4.5. Electrophysiology

Young Wistar rats (age 11–17 days) were decapitated under ether anaesthesia; brains were rapidly removed, placed in oxygenated ice-cold artificial cerebrospinal fluid (ACSF; composition in mM: NaCl 124; KCl 3.0; NaH_2PO_4 1.2; $MgSO_4$ 1.2; $CaCl_2$ 2.0; $NaHCO_3$ 26; D-glucose 10, pH 7.3) and cut into 300 μm slices with a vibratome. One slice containing the hippocampus was then transferred to the recording chamber of a patch-clamp set-up, continually perfused with oxygenated ACSF and viewed under an infrared differential interference contrast microscope (Leica DMLFS). CA1 pyramidal neurons were visually identified by their location and by their typical shape and dimension. Membrane current was recorded from single CA1 pyramidal neurons with the patch clamp technique in the whole-cell configuration, using an L/M-EPC7 amplifier (List Electronic, Germany). The recording electrode was a glass micropipette (resistance 1.5–3 M Ω) filled with intracellular

solution (composition in mM: K-gluconate 170; HEPES 10; NaCl 10; MgCl₂ 2; EGTA 0.2; Mg-ATP 3.5; Na-GTP 1; pH 7.3). Capacitive currents were electronically cancelled and series resistance was compensated by 60–80%. Data were acquired and analysed using EPC and Signal softwares (Cambridge Electronic Design, England). Immediately after the beginning of recording, the slice was perfused with a Mg⁺⁺-free ACSF containing tetrodotoxin (TTX, 1 μ M, Tocris) to prevent synaptic activity. *N*-methyl-D-aspartic acid (NMDA, 50 μ M, Sigma) was dissolved in Mg⁺⁺-free ACSF containing glycine (0.5 μ M, Sigma) and TTX (1 μ M) and was applied during 5 s using a computer-controlled electrovalve solution changer (MSC-200, Bio-Logic). Compound **3d** was dissolved in Mg⁺⁺-free ACSF (containing TTX, 1 μ M) and applied by bath perfusion at a flow rate of 1 mL/min. The holding potential of CA1 pyramidal neurons was set at –60 mV and membrane current was continually recorded at an acquisition rate of 4 KHz. Several pulses of NMDA were applied for each neuron respectively in control conditions and during continuous application of **3d** at different doses (1, 10, and 100 μ M, 5 min) through the bath perfusion system. NMDA-induced current amplitude was measured as the difference between peak current amplitude and baseline. For each neuron studied, the amplitude of at least three consecutive NMDA-induced currents were measured respectively in control conditions and in the presence of compound **3d** and the two sets of raw values were compared using Student's unpaired *t*-test (Graph Pad software). To illustrate the time course of NMDA-mediated current blockade by **3d** (10 μ M), current amplitude values were normalized (dividing by mean amplitude value, calculated from at least three NMDA responses in control conditions); normalized NMDA-mediated currents from all the responsive neurons were pooled (mean \pm SEM) and represented on a graphic as a function of time.

4.6. Automated molecular docking experiments

Prior to docking, the ligand structures were built using standard bond lengths and angles from the Sybyl 8.2 fragment library and fully optimized by the semiempirical quantum mechanical method AM1. The structure of the NR2B ifenprodil-like recognition site was recently reported by us.¹⁹ Automated docking studies were then performed using CCDC GOLD (Genetic Optimization for Ligand Docking) software version 3.1.1.²⁶ A 10.0 radius active site was defined centred on the position of ligand Ro-25,6981, as previously reported.¹⁹ For all calculations GOLD score was chosen as fitness function and the standard default settings were used in all the calculations. For each of the 100 independent genetic algorithm runs, a default maximum of 100,000 genetic operations was performed, using the default operator weights and a population size of 100 chromosomes. Default cutoff values of 2.5 Å for

hydrogen bonds and 4.0 Å for VdW were employed. Results differing by less than 1.5 Å in ligand-all atom RMSD were clustered together.

Acknowledgements

We gratefully acknowledge expert technical assistance at Salvatore Todaro of Dipartimento Farmaco-Chimico—Università di Messina. Financial support for this research by MiUR is gratefully acknowledged.

References and notes

- Paoletti, P.; Neyton, J. *Curr. Opin. Pharmacol.* **2007**, *7*, 39.
- Mayer, M. L. *Curr. Opin. Neurobiol.* **2005**, *15*, 282.
- Chazot, P. L. *Curr. Med. Chem.* **2004**, *11*, 389.
- Marinelli, L.; Cosconati, S.; Steinbrecher, T.; Limongelli, V.; Bertamino, A.; Novellino, E.; Case, D. A. *Chem. Med. Chem.* **2007**, *2*, 1498.
- Malherbe, P.; Mutel, V.; Broger, C.; Perin-Dureau, F.; Kemp, J. A.; Neyton, J.; Paoletti, P.; Kew, J. N. J. *Pharmacol. Exp. Ther.* **2003**, *307*, 897.
- Loftis, J. M.; Janowsky, A. *Pharmacol. Ther.* **2003**, *97*, 55.
- Nikam, S. S.; Meltzer, L. T. *Curr. Pharm. Des.* **2002**, *8*, 845.
- Borza, I.; Kolok, S.; Gere, A.; Nagy, J.; Fodor, L.; Galgoczy, K.; Fetter, J.; Bertha, F.; Agai, B.; Horvath, C.; Farkas, S.; Domany, G. *Bioorg. Med. Chem. Lett.* **2006**, *16*, 4638.
- Borza, I.; Greiner, I.; Kolok, S.; Galgoczy, K.; Ignacz-Szendrei, G.; Horvath, C.; Farkas, S.; Gati, T.; Hada, V.; Domany, G. *Pharmazie* **2006**, *61*, 799.
- Borza, I.; Domany, G. *Curr. Top. Med. Chem.* **2006**, *6*, 687.
- McCauley, J. A. *Exp. Opin. Ther. Patent* **2005**, *15*, 389.
- McCauley, J. A.; Theberge, C. R.; Romano, J. J.; Billings, S. B.; Anderson, K. D.; Claremon, D. A.; Freidinger, R. M.; Bednar, R. A.; Mosser, S. D.; Gaul, S. L.; Connolly, T. M.; Condra, C. L.; Xia, M. H.; Cunningham, M. E.; Bednar, B.; Stump, G. L.; Lynch, J. J.; Macaulay, A.; Wafford, K. A.; Koblan, K. S.; Liverton, N. J. *J. Med. Chem.* **2004**, *47*, 2089.
- Barta-Szalai, G.; Borza, I.; Bozo, E.; Kiss, C.; Agai, B.; Prosenyak, A.; Keseru, G. M.; Gere, A.; Kolok, S.; Galgoczy, K.; Horvath, C.; Farkas, S.; Domany, G. *Bioorg. Med. Chem. Lett.* **2004**, *14*, 3953.
- Claiborne, C. F.; McCauley, J. A.; Libby, B. E.; Curtis, N. R.; Diggle, H. J.; Kulagowski, J. J.; Michelson, S. R.; Anderson, K. D.; Claremon, D. A.; Freidinger, R. M.; Bednar, R. A.; Mosser, S. D.; Gaul, S. L.; Connolly, T. M.; Condra, C. L.; Bednar, B.; Stump, G. L.; Lynch, J. J.; Macaulay, A.; Wafford, K. A.; Koblan, K. S.; Liverton, N. J. *Bioorg. Med. Chem. Lett.* **2003**, *13*, 697.
- Menniti, F. S.; Pagnozzi, M. J.; Butler, P.; Chenard, B. L.; Jaw-Tsai, S. S.; White, W. F. *Neuropharmacology* **2000**, *39*, 1147.
- Chenard, B. L.; Menniti, F. S. *Curr. Pharm. Des.* **1999**, *5*, 381.
- Gogas, K. R. *Curr. Opin. Pharmacol.* **2006**, *6*, 68.
- Kosowski, A. R.; Liljequist, S. J. *Pharmacol. Exp. Ther.* **2004**, *311*, 560.
- Gitto, R.; De Luca, L.; Ferro, S.; Occhiuto, F.; Samperi, S.; De Sarro, G.; Russo, E.; Ciranna, L.; Costa, L.; Chimirri, A. *Chem. Med. Chem.* **2008**, *3*, 1539.
- Chapman, A. G.; Croucher, M. J.; Meldrum, B. S. *Arzneimittelforschung* **1984**, *34*, 1261.
- Advanced; Chemistry; Development. www.acdlabs.com/.
- Ciranna, L.; Cavallaro, S. *Exp. Neurol.* **2003**, *184*, 778.
- Galvez, C.; Viladoms, P. J. *Heterocycl. Chem.* **1982**, *19*, 665.
- Litchfield, J. T., Jr. *J. Pharmacol. Exp. Ther.* **1949**, *97*, 399.
- MDS pharma services, T. <http://www.mdsps.com/>.
- Jones, G.; Willett, P.; Glen, R. C.; Leach, A. R.; Taylor, R. J. *Mol. Biol.* **1997**, *267*, 727.